Journal of Constructional Steel Research 99 (2014) 111–120

Contents lists available at ScienceDirect

Journal of Constructional Steel Research

Studying the seismic behavior of gate braced frames by incremental dynamic analysis (IDA)

N. Fanaie *, S. Ezzatshoar

K.N. Toosi University of Technology, Tehran, Iran

ARTICLE INFO

Article history:
Received 30 May 2013
Accepted 2 April 2014
Available online xxxx

Keywords:
Gate bracing
Response modification factor
Overstrength factor
Ductility factor and incremental dynamic analysis

ABSTRACT

This paper critically evaluates overstrength, ductility and response modification factors of steel frames with gate bracing. Gate bracing system is a kind of concentric bracing systems. It is similar to chevron (inverted V) bracing except that its diagonal members are not straight. The members of different slopes are joined together at a point to provide enough space for openings.

In order to achieve the purpose of this research, several buildings of different stories are considered on soil type II. Static pushover analysis, linear dynamic analysis and nonlinear incremental dynamic analysis are performed by OpenSees software concerning 10 records of past earthquakes. Also, ductility factor, overstrength factor and response modification factor have been calculated for gate bracing system. The values of 3.5 and 5 are suggested for response modification factor in ultimate limit state and allowable stress methods, respectively. The fragility curves were plotted for the first time for such kind of braces. It should be mentioned that these curves play significant roles in evaluating seismic damage of buildings.

1. Introduction

Nowadays, concentric and eccentric bracings are the most common bracings used for strengthening the structures against seismic lateral loads. The usual forms of concentric bracings cause some problems in providing the spaces needed for openings in the structures. Accordingly, in recent years, architects have suggested a new type of bracing known as gate bracing.

Presently, gate bracing is used more frequently in low and middle rise buildings in Iran. As a result of its frequent use, several researchers have focused on these braces to calculate their in-plane and out of plane buckling loads as well as other seismic parameters. However, no comprehensive research has been done based on accurate nonlinear dynamic analysis concerning the seismic response of these braces against real earthquake accelerograms. Response modification factor is one of most important parameters in assessing the seismic behavior of structures. It shows the non-elastic performance of structures and its hidden resistance in the non-elastic behavior stage.

In different codes, response modification factor is obtained for any structural system based on the ductility (R_{μ}) and overstrength (R_s) of structures. The concept of response modification factor was presented for the first time based on the ductility, overstrength and indeterminacy of structures for calculating the least design base shear, presented in ATC-3-06 [1] and modified in ATC-19 [2] and ATC-34 [3].

The initial values suggested for R factor were primarily based only on the limited experiences and engineering judgments. It means that no accurate numerical or analytical methods, indicating a physical event, had been presented since then. However, nowadays, response modification factor is mainly calculated for different structural systems based on the concepts of ductility and overstrength.

This study focuses on evaluating the overstrength, ductility and response modification factors and presents the fragility curves of gate braced steel frames. The frames were designed based on the Iranian Code for seismic design (Standard No. 2800) and Iranian National Building Code (part 10) for Structural Steel Design [5]. Also, nonlinear static pushover, nonlinear incremental dynamic and linear dynamic analyses have been carried out to capture the purpose.

2. Gate bracing system

Gate bracing is similar to inverse V chevron bracing; the only difference is that its inverse V members are fractured in order to provide more openings. The fractured points are connected to the beam-column connection point with another bracing member. Gate bracing is better than concentric bracing because it provides wider architectural openings. However, the values of stiffness, strength and ductility are lower in gate bracing compared to those of concentric bracing. A sample of gate bracing is shown in Fig. 1. The point, where the bracing members

* Corresponding author at: K.N. Toosi University of Technology, Civil Engineering Department, No. 1346, Vali-Asr Street, P.O. Box. 15875-4416, 19697 Tehran, Iran. Tel.: +98 21 8877 9623.

E-mail addresses: fanaie@kntu.ac.ir (N. Fanaie), s_ezatshoar@sina.kntu.ac.ir (S. Ezzatshoar).

http://dx.doi.org/10.1016/j.jcsr.2014.04.008
0143-974X/

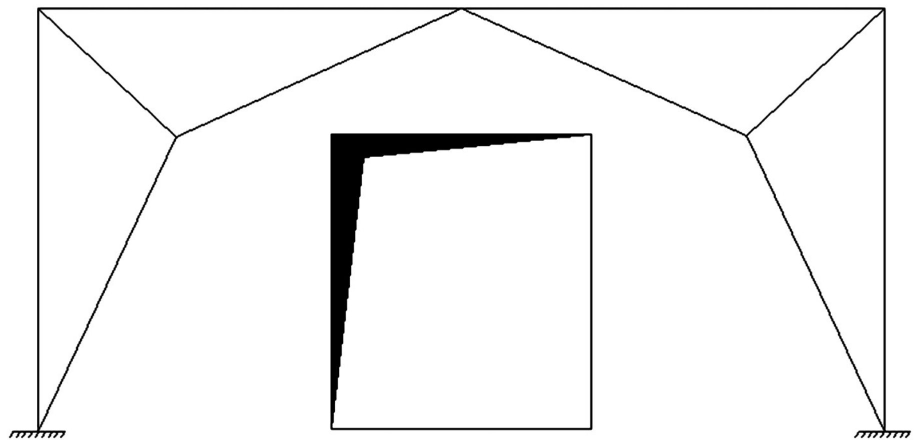

Fig. 1. Frame with gate bracing.

are joined together, will determine the size of the openings of the structure. The more the joint location moves towards the beam-column connection point, the larger are the openings created.

The connection of beam and column together and their connection to the bracings are both assumed simple in most braced frames. However, this assumption in connecting three diagonal members together will cause the frame's geometrical instability against lateral forces normal to the plane of the frame. Therefore, the connection should have enough flexural stiffness in the junction of the 3 bracing members for resisting out of plane buckling. Regarding this condition, the bracings are not truss members in the direction vertical to the frame's plane; they behave as beam column members [6].

Assuming enough stability in the out of plane direction and continuity of beam in the joint C, the structure collapses because of buckling of compression members and plastic hinge formation in joint C [6]. This phenomenon is presented in Fig. 2.

Compressional braces may experience out of plane buckling under lateral forces. This results in the movement of joint connection from the frame's plane.

The empirical studies conducted by Building and Housing Research Center (BHRC) show that this kind of bracing is crucial in determining the out of plane buckling of compressive members [7]. Such buckling is prevented by designing the sections in such a way that the value of gyration radius is higher in the out of plane buckling compared to that of in-plane buckling. Moreover, locating the convergence point at a distance of 0.25 of the braced panel diameter from the frame's corner can provide optimum stiffness and strength of lateral system. Besides, these braces can be designed and applied if the connections are performed appropriately in the middle point to provide enough stiffness [8].

3. Incremental dynamic analysis (IDA)

3.1. Introduction of IDA

The random nature of earthquakes is one of the main sources of uncertainty in assessing the seismic behavior of structures. In quantifying such uncertainties, the seismic response of structures should be determined for different earthquake records using different dynamic analyses [9]. In this study, earthquake uncertainty was studied using incremental dynamic analysis (IDA). In this regard, sufficient numbers of records are used to consider the uncertainties in the frequency content and spectral shapes of earthquakes. Each record is scaled in such a way as to cover appropriate ranges of seismic intensities and structural responses from elastic limit to collapse.

In IDA, the intensity measure (IM) (PGA or S_a (T_1)) is scaled with a proper algorithm from a very low amount to a certain level in order to motivate the elastic response and target collapse state respectively. Time history analysis is conducted in IDA using different records generated by various scaling factors. Different values of damage measure (DM) are calculated at the end of each analysis. These values correspond to the IM levels used in dynamic analysis. Finally, a response curve (IDA

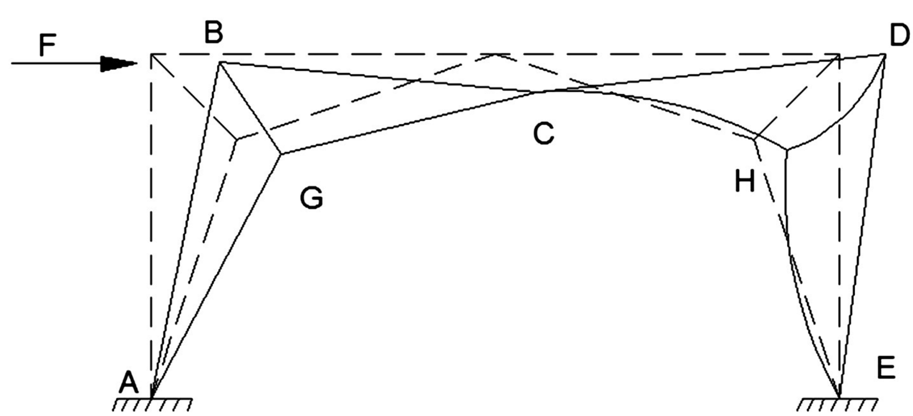

Fig. 2. Nonlinear deformation in gate bracing.

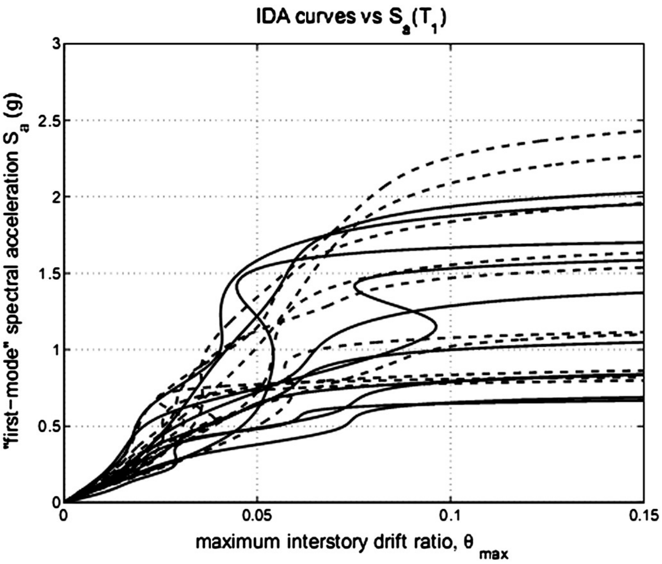

Fig. 3. $S_a(T_1)$ curve vs. DM.

curve) is drawn by plotting DM against intensity for each scaled record as shown in Fig. 3.

The procedure given below is followed for all considered records:

- the concerned damage limit states are denoted;
- the IDA curves are plotted and interpreted properly;
- the performances and responses of the structure, subjected to certain conditions, are studied;
- the capacity point is found.

3.2. Intensity measure (IM) scale

It is very important to select appropriate parameters for IM and DM in IDA analysis. These parameters should be scalable in order to be selected for a proper seismic intensity. They should also have the dynamic characteristics of each record such as frequency content, energy and so on. Consequently, the structural responses will vary slightly under different earthquake records [9]. In this study, the spectral acceleration of the first mode was selected as seismic intensity parameter in order to include the principal period time of the structure in the scaling and consider the earthquake's duration and damping parameters.

3.3. Damage measure (DM) criterion

DM is a positive scholar quantity derived from nonlinear dynamic analysis output. Maximum base shear, node rotations, inter-story drift and axial deformation of the elements can be considered as the damage measure criteria. The proper damage measure criterion is selected based on its application and also, based on the structure. In the shear buildings, maximum inter-story drift ratio is correlated properly with the joint rotations as well as local and global damages of the structure. Therefore, it can be considered as a very good option for DM [9].

In this study maximum inter-story drift was used as DM to achieve appropriate structural response against the earthquake records.

3.4. Choosing and scaling of accelerograms

The accelerograms of considered earthquakes were selected for IDA. The parameters of these events are very similar to those of the site on which the structure has been built. Accordingly, 10 records are chosen

Table 1
Characteristics of earthquake records used for IDA analysis.

Record	Station	Earthquake date	PGA (g)
Chi-Chi, Taiwan	CHY080	09/20/1999	0.902
Coyote Lake	Gilroy Array 3	08/06/1979	0.434
Kobe	KJMA	01/16/1995	0.821
Landers	Cool water	06/28/1992	0.417
Loma Prieta	Corralitos	10/18/1989	0.644
Morgan Hill	Anderson Dam	04/24/1984	0.423
N. Palm Springs	N. Palm Springs	07/08/1986	0.694
Northridge	Santa Monica	01/17/1994	0.883
Bam	Bam	26/12/2003	0.767
Tabas	Tabas	09/16/1978	0.917

from famous worldwide earthquakes including two big earthquakes in Iran, Bam and Tabas as listed in Table 1. Shear wave velocities of all these sites correspond to the velocity in soil type II as presented by Iranian code for seismic design (Standard No. 2800)[4] and site category B of USGS classification.

Regarding IM scaling, hunt and fill algorithm was used to optimize the number of scaling of each record. They are applied in nonlinear dynamic analysis and drawing IDA curves with enough accuracy and speed [9]. In the first step of IM scaling, a very low level of seismic intensity parameter (0.005 g) is selected (spectral acceleration of the first mode) which guarantees the linear response of structure. A minimum number of points are used in the hunt stage in order to achieve the range of spectral acceleration of the first mode where the damage has happened. Based on Eq. (1), the IM values increase sequentially with the seismic intensity in each step. The value of $S_a(T_1)$ in each step is calculated as follows:

$$S_a(T_1)_i = S_a(T_1)_{i-1} + \alpha \times (i-1) \tag{1}$$

where, $S_a(T_1)$ is spectral acceleration corresponding to the first mode; i is the number of steps; and α is a factor. In this research $\alpha = 0.05$.

Fill step is started after analyzing each step and finding the interval of spectral acceleration where the damage limit state happens. As the seismic stress parameter increases progressively, it is observed that it increases in accordance with the above relation. In this step, the spectral acceleration which accurately corresponds to the considered damage

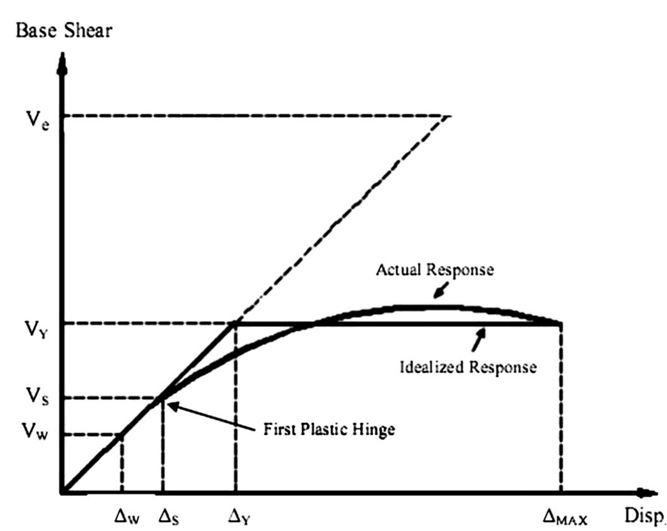

Fig. 4. Nonlinear behavior of structure.

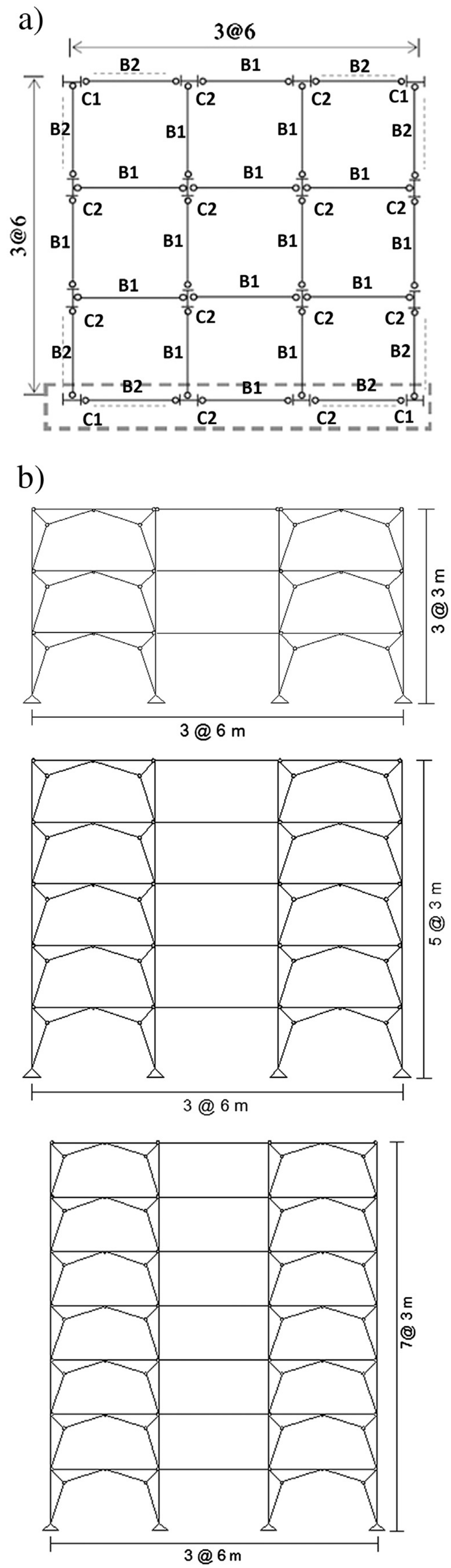

Fig. 5. Configuration of model structure. (a) Plane. (b) Brace configuration.

Table 2
Cross sections of models members.

Structure	Story	C1	C2	B1	B2	Brace
3 story	1	IPB 180	IPB 200	IPE 330	IPE 400	2UNP 140
	2	IPB 180	IPB 200	IPE 330	IPE 400	2UNP 120
	3	IPB 160	IPB 180	IPE 300	IPE 360	2UNP 120
5 story	1	IPB 200	IPB 220	IPE 330	IPE 400	2UNP 200
	2	IPB 200	IPB 220	IPE 330	IPE 400	2UNP 200
	3	IPB 180	IPB 200	IPE 330	IPE 400	2UNP 160
	4	IPB 180	IPB 200	IPE 330	IPE 400	2UNP 160
	5	IPB 160	IPB 180	IPE 300	IPE 360	2UNP 140
7 story	1	IPB 240	IPB 260	IPE 330	IPE 400	2UNP 240
	2	IPB 240	IPB 240	IPE 330	IPE 400	2UNP 220
	3	IPB 220	IPB 240	IPE 330	IPE 400	2UNP 220
	4	IPB 180	IPB 200	IPE 330	IPE 400	2UNP 200
	5	IPB 180	IPB 180	IPE 330	IPE 400	2UNP 180
	6	IPB 160	IPB 180	IPE 330	IPE 400	2UNP 140
	7	IPB 160	IPB 160	IPE 300	IPE 360	2UNP 140

limit state is determined by increasing the analysis points between two spectral acceleration values where the considered damage limit state happens. The accuracy of IDA curve can also increase by increasing the analysis points in other intervals of spectral acceleration of the first mode.

3.5. Determination of failure criteria

Different codes such as FEMA and rehabilitation standards have suggested diverse criteria for damage determination in different limit states. These criteria have been presented by FEMA350 for special moment resistant frames as follows:

- Inter-story drift ratio of 2% equivalent to the level of immediate occupancy (IO). In this performance level, the structure can be used uninterruptedly as its strength and stiffness are not changed significantly.
- Inter-story drift ratio of 10% with respect to a resistance factor of 0.85, equivalent to the level of collapse prevention (CP) for mid-rise buildings. In this performance level, the building is damaged greatly but not collapsed [10].

In this research, the concept of inter-story drift ratio has been used. The failure criteria were defined in the two following levels:

3.5.1. Drift of floors

The maximum drift was selected for immediate occupancy (IO) level based on the Iranian Standard No. 2800 as follows [4]:

(a) For the frames with the fundamental period less than 0.7 s:

$$\Delta < 0.025H \tag{2}$$

(b) For the frames with the fundamental period more than 0.7 s:

$$\Delta < 0.02H \tag{3}$$

where, H is height of story.

3.5.2. Failure mechanism and frame instability

To determine the ultimate limit, defined by maximum inter-story drift ratio, the frame should keep its stability. In case of occurring

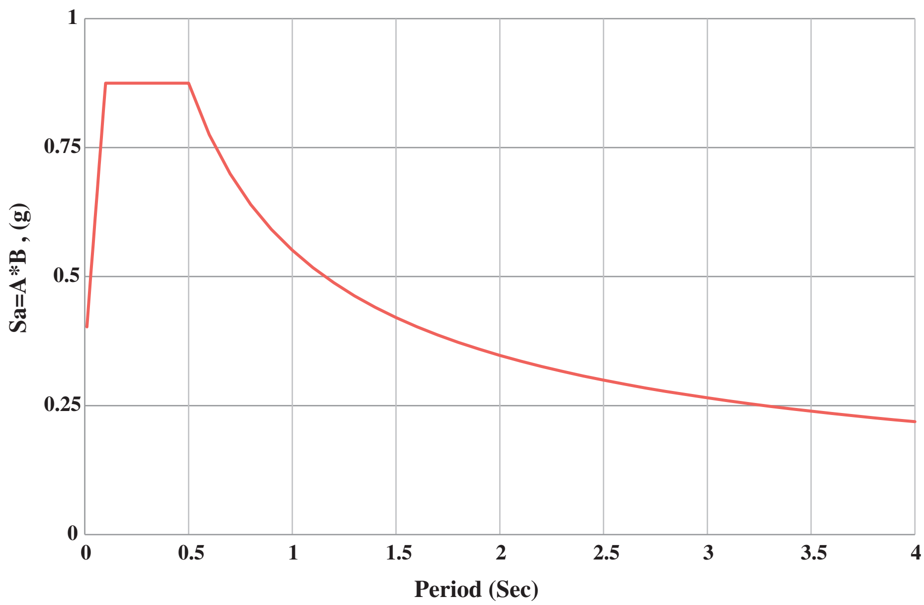

Fig. 6. Variation of spectral acceleration with period of structure.

story mechanism, nonlinear dynamic analysis is stopped. Hence, the last scaled earthquake base shear is selected as ultimate limit state.

4. Calculating response modification factor

4.1. Basis of calculating response modification factor

Since the end of the 80s, several researchers have been working on different methods of calculating response modification factor and the factors that affect it. The most remarkable of these methods is ductility factor method presented by Prof. Yang [11]. In this method, the actual nonlinear behavior of the structure is modeled through a bilinear graph.

In the mentioned graph, V_y is the yielding force and V_e is the maximum base shear when behavior of the structure and assumed to be linear during an earthquake. V_e is reduced to V_y due to the ductility and nonlinear behavior of the structure as shown in Fig. 4.

Force reduction factor is defined as follows:

$$R_{\mu} = V_e/V_y \tag{4}$$

Overstrength factor is the ratio of base shear of mechanism formation (V_y) to the base shear of the first plastic hinge formation in the

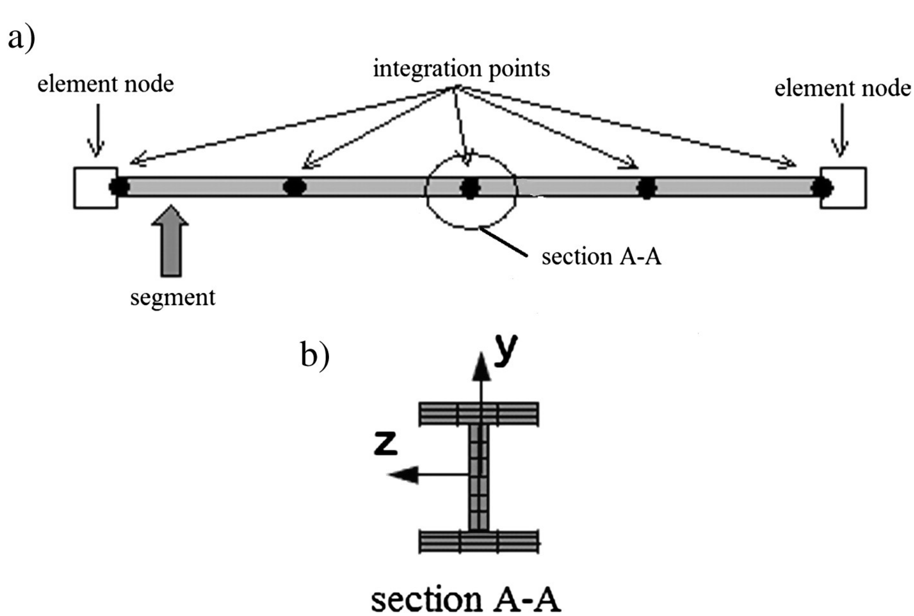

Fig. 7. Schematic division of element and section into segment and fiber elements in OpenSees. a) Dividing the element into several segments. b) Dividing the section into fiber elements.

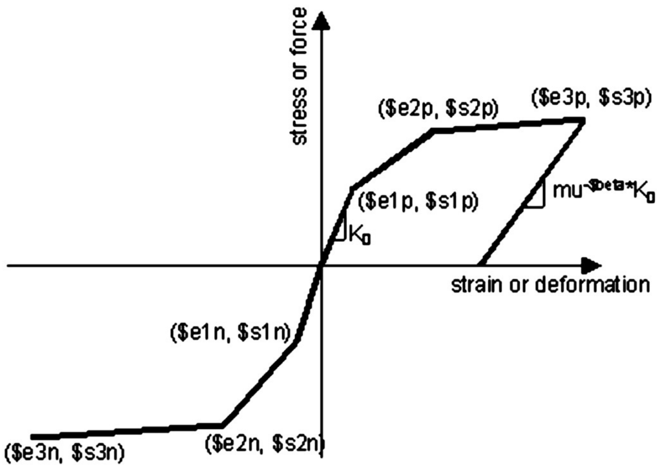

Fig. 8. The behavior of hysteric material model [16].

structure (V_s) (the occurrence of the first yielding in the elements) and defined as follows [11]:

$$R_s = V_y / V_s \tag{5}$$

Overstrength factor is based on using nominal material properties and called R_{so}. Some other effects are also considered in actual overstrength factor (R_s) and defined as follows [11]:

$$R_s = R_{so} \times F_1 \times F_2 \ldots F_n \tag{6}$$

where, F is used for calculating the difference between actual and nominal static yield strengths and F_2 for considering the increase of yield stress as a result of strain rate effect during an earthquake.

In this research, the product of F1 and F2 has been considered as 1.1. This value is recommended by the reference [11] as well as Iranian National Building Code (part 10).

Other parameters can also be included when reliable data is available. They are included in parameters such as nonstructural component contributions and variation of lateral force profile.

Based on the design codes, V_s is reduced to V_w in designing with allowable stress method and defined as follows:

$$\gamma = V_s / V_w \tag{7}$$

This factor is 1.4–1.5 for wide flange profiles. Allowable stress factor is taken as 1.44 in this research based on the recommendations of UBC-97 [12].

Regarding the above explanations, response modification factor is used for converting the linear force applied to the structure to designing force. It is applied in the allowable stress design and ultimate strength methods using Eqs. (8) and (9), respectively [11]:

$$R = \left(V_e / V_y\right) \times \left(V_y / V_s\right) \times \left(V_s / V_w\right) = R_\mu \times R_s \times \gamma \tag{8}$$

$$R = \left(V_e / V_y\right) \times \left(V_y / V_s\right) = R_\mu \times R_s \tag{9}$$

4.2. Calculating overstrength factor by incremental nonlinear dynamic analysis

This method was presented by Mwafy and Elnashai [13] and is used for calculating base shear through IDA. Overstrength factor is the ratio of final base shear to base shear corresponding to the first yielding. Based on the reference [14], this method is modified as follows:

$$R_s = V_{b(Dyn,y)} / V_{b(St,s)} \tag{10}$$

where, R_s is overstrength factor, $V_{b(Dyn,y)}$ is dynamic base shear and $V_{b(St,s)}$ is static base shear corresponding to the first yieldingin the structure.

$V_{b(St,s)}$ is used because there may be only one plastic hinge in the structure. In case of a second hinge formation during gradual increase

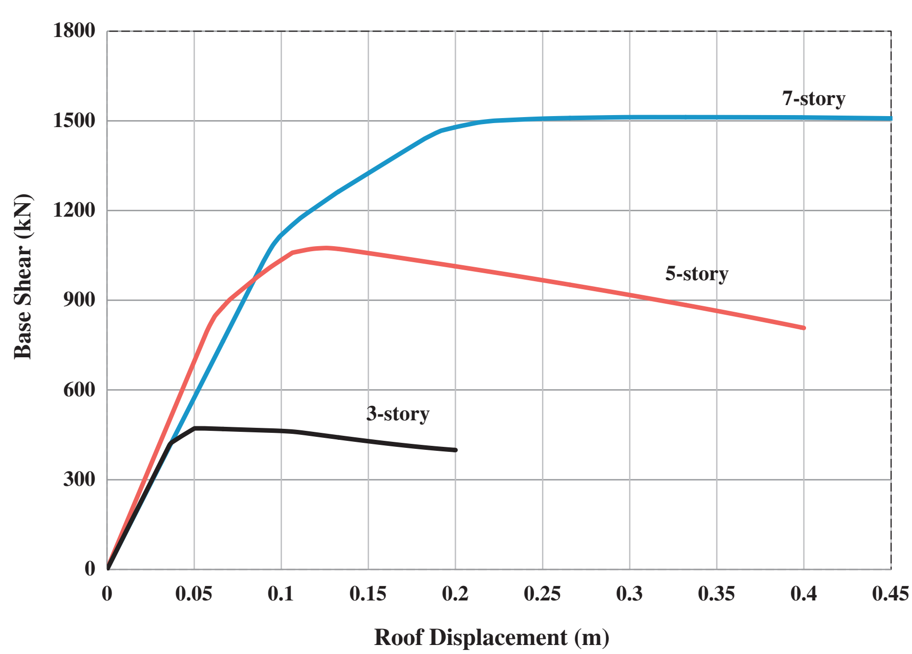

Fig. 9. Pushover curves of studied frames.

Table 3
First hinge base shear of models.

No. of story	Vs (KN)
3	414.6
5	794.27
7	1028.3

of spectral acceleration, there would still be just one plastic hinge in the whole structure. In such cases, the point of the first yielding cannot be distinguished easily. Therefore, the base shear which corresponds to the first plastic hinge formation, derived from nonlinear static analysis, is used as base shear of yielding point. It means that the end of the linear zone can be considered the same in both pushover and IDA curves [13, 14].

4.3. Calculating the ductility factor

Maximum nonlinear base shear ($V_{b(Dyn,y)}$) which corresponds to the target limit state is obtained by IDA using the scaled earthquake records. After that, maximum linear base shear ($V_{b(Dyn,e)}$) is calculated by elastic analysis of the structure under the same records. Ductility factor is computed according to the below formula:

$$R_{\mu} = V_{b(Dyn,e)}/V_{b(Dyn,y)} \tag{11}$$

5. The studied models

Gate bracings have lower ductility compared to other concentric braces [15] hence; they are used in the low and mid-rise as well as residential buildings to provide the spaces needed for openings.

In this research, three steel frames of 3, 5 and 7 stories with bracing systems have been studied according to the Iranian standard No. 2800. They have been assumed to be established in a zone with very high seismicity on the soil type II (based on the Iranian standard No. 2800) with an average shear wave velocity of 360–750 m/s^2 in a depth of 30 m. These buildings have been designed in line with the requirements of Iranian earthquake resistance design code [4] and Iranian National Building Code (part 10) for steel structure design [5].

The heights of all stories are 3 m, the spans are 6 m and the applied steel is of st-37-1 kind (which is equivalent to the steelS235 based on the standard EN10025) with a yield stress of 235 Mpa. The dead and live loads are 4.5 kN/m^2 and 2 kN/m^2, respectively. All connections including beam to column, braces to each other and braces to beam-column joint are in the form of hinge. However, the connections of the three bracing members should have sufficient rigidity at their crossing point in order to resist against the movements normal to frame plane and prevent geometric instability.

In order to consider the out of plane buckling effect in such bracing, the effective length factor has been considered as 1.6 [8]. This effective length factor is obtained based on the works of Saffari and Mosalman Yazdi [8] conducted on the analysis of out of plane buckling in such bracing, including their figures.

The above obtained effective length factor is considered for designing the braces. Middle Gusset plate is used in the both sides of the connection node with sufficient thickness. Enough welding length is provided in connecting the bracing members to each other. If there is sufficient rigidity between the connection nodes of bracings for moving normal to the plane, the probability of out of plane buckling of the frames is also dramatically reduced accordingly out of plane buckling always happens after in plane buckling. Therefore, in plane instability mode will be the dominant damage mode.

The formation of plastic hinge is due to the effect of general buckling of the brace in the plane and its yielding under tensional or compressive

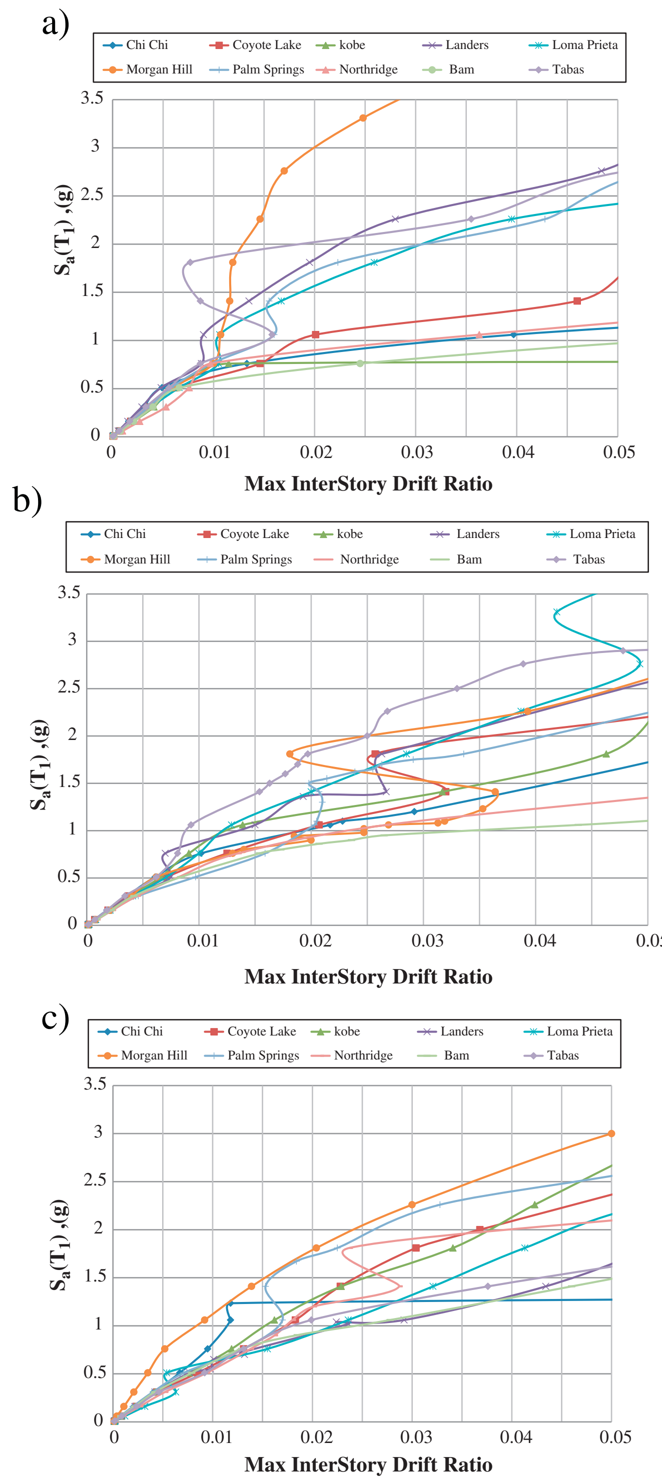

Fig. 10. Incremental dynamic analysis results for (a) 3 story, (b) 5 story and (c) 7 story.

axial forces. Therefore, it is not needed to input directly the effects of out of plane buckling in the analysis.

In this study, the plans of all stories have been considered the same and shown in Fig. 5. The locations of bracings are presented as dotted line in this figure. Due to the fact that the internal frames have totally hinged connections without bracings, they play no role in tolerating the lateral loads. A two-dimensional frame has been selected as the representative of the tri-dimensional structure for IDA analysis in order to reduce the time and calculation volume

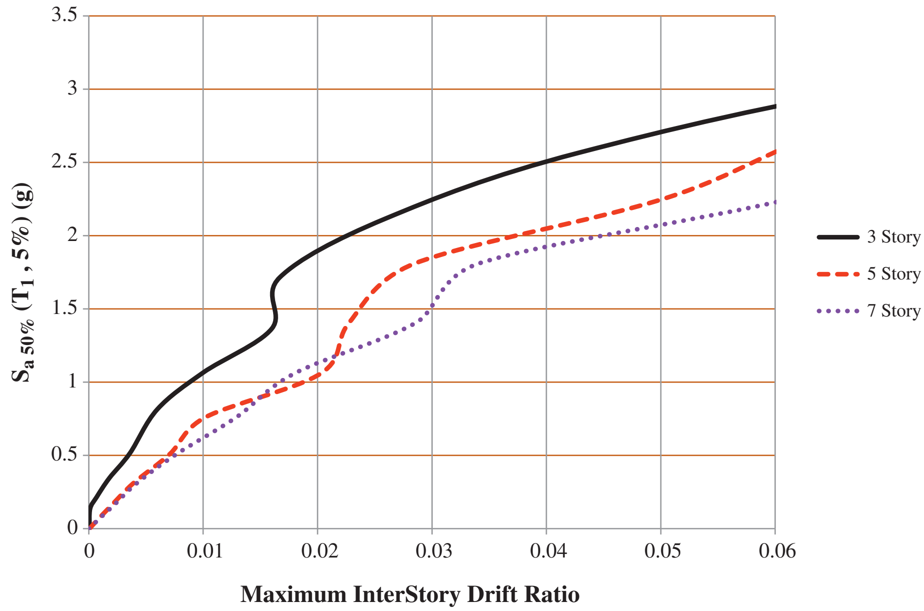

Fig. 11. Median IDA curves.

of dynamic analysis. The mentioned frame has been shown by dotted line in the above mentioned figure. The cross-sections of model members are shown in Table 2.

In order to design the structures subjected to earthquake, equivalent lateral static forces were applied to all stories. These forces are calculated according to the Iranian Earthquake Code (Standard No. 2800) [4]. The design base shear is computed as follows:

$$V = C \times W \tag{12}$$

$$C = (A \times B \times I)/R \tag{13}$$

where, V is base shear; C is seismic coefficient; W is equivalent weight of structure; A is design base acceleration; B is response factor; I is importance factor; and R is response modification factor. $A \times B$ is design spectral acceleration expressed as gravitational acceleration (g) against fundamental period of structure (T) for soil type II as presented in Fig. 6.

The importance factor (I) and design base acceleration (A) were assigned with the values of 1 and 0.35, respectively, for designing the frames.

The value of primary response modification factor is taken as 5.5 in allowable stress design method because the gate bracings have lower ductility compared to other concentric braces [15].

The frame members have been designed by allowable stress design method according to Iranian National Building Code (part 10).

6. OpenSees software

The OpenSees 2.2.1 was used for modeling and conducting incremental dynamic analysis. This software, produced by Berkley University of California, is one of the most effective software in nonlinear and dynamic analysis [16].

For modeling the members in nonlinear range of deformation, the following assumptions were made. Nonlinear beam-column element is used in the software to model the columns, beams and bracings. This element can consider the effects of P-Δ and large deformations to account for geometric nonlinear effect of the model.

In order to model wide plasticity in the member length and nonlinear buckling in the program, each element including beam, column and bracing, is divided into several fibers along their sections and several segments along their lengths.

The schematic configurations of these segments and fiber elements are presented in Fig. 7. The elements have been divided into 10 parts in their lengths for the purpose of being modeled in the program as well as increasing the analysis accuracy. The web and flange of each steel section applied in the models have been divided into 6–

Table 4
Nonlinear maximum base shear and limit state point for models under ground motions.

Records	3-story			5-story			7-story		
	Limit state	S_a (g)	$V_{b\ (Dyn,y)}$ (kN)	Limit state	S_a (g)	$V_{b\ (Dyn,y)}$ (kN)	Limit state	S_a (g)	$V_{b\ (Dyn,y)}$ (kN)
Chi Chi	Drift 2.5%	1.008	529.98	Drift 2.5%	1.134	1171.66	Drift 2%	1.235	1328.16
Coyote Lake	Drift 2.5%	1.126	540.66	Drift 2.5%	1.193	1181.67	Drift 2%	1.192	1254.59
Kobe	Drift 2.5%	1.016	511.95	Drift 2.5%	1.278	1185.56	Drift 2%	1.259	1245.77
Landers	Drift 2.5%	2.101	530.18	Drift 2.5%	1.399	868.75	Drift 2%	0.720	1043.23
Loma Prieta	Drift 2.5%	1.771	513.89	Drift 2.5%	1.645	1122.23	Drift 2%	0.927	1533.20
Morgan Hill	Drift 2.5%	3.320	503.71	Drift 2.5%	1.025	979.27	Drift 2%	1.810	1278.26
Palm Springs	Drift 2.5%	1.869	563.35	Drift 2.5%	1.657	1176.15	Drift 2%	1.725	1379.75
Northridge	Drift 2.5%	0.933	505.26	Drift 2.5%	1.021	1085.14	Drift 2%	1.193	1299.62
Bam	Drift 2.5%	0.764	497.09	Drift 2.5%	0.950	1190.60	Drift 2%	0.928	1491.50
Tabas	Drift 2.5%	2.090	523.21	Drift 2.5%	2.000	998.51	Drift 2%	1.062	1178.64
$V_{b\ (Dyn,y),\ ave}$ (kN)			521.93			1095.95			1303.27

Table 5
Linear maximum base shear of models under ground motions.

Records	$V_{b(Dyn,e)}$ (KN)		
	3-story	5-story	7-story
Chi Chi	897.47	2382.83	3450.57
Coyote Lake	1114.48	2569.74	3115.80
Kobe	1197.68	2635.99	3139.94
Landers	1708.22	2834.57	1964.23
Loma Prieta	1645.26	2594.71	3316.05
Morgan Hill	2074.98	2112.34	2443.31
Palm Springs	1797.51	2362.10	2930.44
Northridge	1143.07	3179.46	4168.16
Bam	766.51	2189.57	2674.91
Tabas	1935.97	3950.97	2723.16
$V_{b(Dyn,\ e),\ ave}$ (KN)	1428.11	2681.23	2992.66

Table 6
Overstrength, ductility factor and response modification factor of model.

No. of story	R_{so}	R_s	R_μ	γ	R_{ASD}	R_{LRFD}
3	1.258	1.384	2.73	1.44	5.44	3.78
5	1.383	1.521	2.44	1.44	5.35	3.71
7	1.267	1.394	2.29	1.44	4.60	3.19
Average	1.303	1.433	2.487	1.44	5.13	3.56

10 fiber elements along the length of web or flange based on their dimensions.

The behavioral model of uniaxial hystertic material has the capability of modeling steel behavior in the form of tri-linear in tension and compression; this model has been used in modeling steel material. The stiffness slope of steel in tension has been considered as 2% of that of the elastic zone. The behavior model of the material has been depicted in Fig. 8.

Zero-length element has been used at the connections of beam to column as well as bracings to beam and column in order to model the hinge joints of the frame elements and columns bases. The nodes at the hinge joint have been fixed only at the transitional degrees of freedom.

The story masses have been put in the story levels for dynamic analysis considering rigid diaphragms action. Fiber section has been used for each member. An initial mid span imperfection of 1/1000 of the length has been considered for all columns for considering the geometric nonlinearities [17]. P-delta and large geometric nonlinear deformation effects are considered by using corotational transformation of geometric stiffness matrix in the program [16].

7. The analytical results

7.1. Non-linear static analysis

Pushover curves of the frames with different stories were plotted for loading pattern of the first mode in terms of roof displacement-base share and shown in Fig. 9.

The values of static base shear equivalent to the first plastic hinge formation in the structure have been derived from Fig. 9. They are summarized in Table 3 for the frames with different stories.

7.2. IDA curves

IDA curves of the studied frames have been presented in Fig. 10 in terms of maximum inter-story drift ratio-spectral acceleration. All behavior stages of the structure, subjected to earthquake, from elastic limit to collapse and global instability are shown in the curves. The median values have also been plotted for the studied frames and shown in Fig. 11. As it is seen in the curves, the structures enter into the nonlinear zone sooner with increasing the heights. Moreover, the IM values are reduced in the curves for a constant value of DM. In other words, the S_a capacity of structures corresponding to a certain damage criterion is reduced with increasing the height of structure.

7.3. Response modification factor

Ultimate base shear ($V_{b(Dyn,y)}$) and limit state are obtained from nonlinear dynamic analysis. They are tabulated in Table 4 under the earthquake records selected for designed braced frames. Table 5

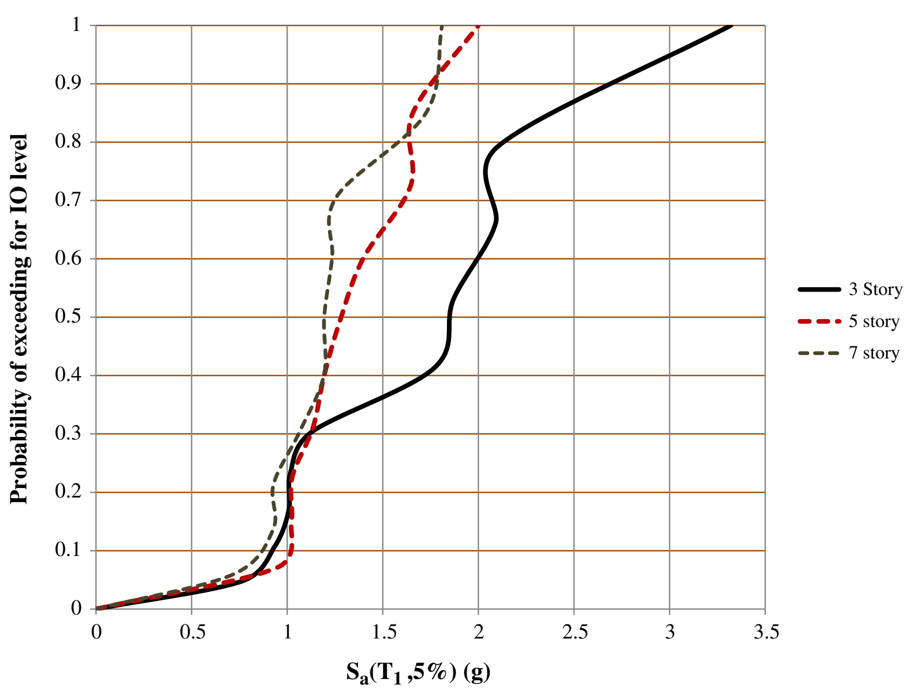

Fig. 12. Fragility curves of the structures with different heights for performance level of Immediate Occupancy (IO).

Table 7
The values of Sa, corresponded to 50% of structural failure.

No. of story	$(Sa\ (T1,5\%))_{IO}$, (g)	Limit state
3	1.84	Drift 2.5%
5	1.28	Drift 2.5%
7	1.19	Drift 2.0%

shows the maximum elastic base shear ($V_{b(Dyn,\ e)}$) resulting from linear dynamic analysis under the selected earthquake records.

Concerning the above results and the descriptions of limit state and allowable stress designing methods in Section 4, ductility, overstrength and response modification factors have been calculated for the studied frames and presented in Table 6. The values obtained for overstrength of the frames are 1.2–1.5.

According to Table 6, the values of overstrength, ductility and response modification factors decrease as the height of building increases. In the shorter frames, the slope of structural behavior curve tends to increase the pre-yield stiffness of the system sharply and thereby reduce the value of $\Delta_{y,}$ as seen in Fig. 4. The specified global drift limit (Δ_{max}) however remains constant at 2% or 2.5% of the height of the system. This in turn greatly increases the ductility and consequently R value of the braced system. In the taller frames, the increase in ductility and R value are of lower magnitudes.

7.4. Plotting the fragility curves

In this research, the fragility curves are used to derive the occurrence probability of the limit state from IDA results. The processes involved in plotting these curves are: first, the IM values which correspond to the considered limit state occurrence are sorted in descending order for all records; second, the occurrence probability of the limit state is calculated for values lower than or equal to the considered IM value. These curves show the occurrence probability of the limit state for each IM value at any performance level of the structure regardless of the seismic hazard. The only condition is that the density value is limited to the considered level [9].

The fragility curves of the limit states of IO have been plotted for all three studied structures and presented in Fig. 12. The values of S_a corresponding to 50% of structural failures were calculated for IO level and presented in Table 7. The values given in this table can be used for designing earthquakes with the probability of certain level of collapse and evaluating the design codes of structures against such earthquakes.

8. Conclusion

In this paper, response modification, ductility and overstrength factors have been calculated for gate bracings. In this regard, three frames of different stories have been subjected to 10 well known global earthquakes and analyzed through IDA and non-linear static analysis. The fragility curves have been plotted for such bracings as well.

Concerning the selected models and records for analysis on the soil with approximately medium shear wave velocity, the obtained results can be considered valid for buildings with medium heights (close to 10 stories) in the regions with high seismicity and semi-stiff soil. The result obtained for gate braced frames in this study can be summarized as follows:

1. The value of overstrength factor is 1.43;
2. The ductility factor value is 2.48;
3. The values of response modification factor are 3.5 and 5 for ultimate limit state method and allowable stress method, respectively;
4. The fragility curves have been plotted for the gate bracings for the first time. These curves can be used as the bases for estimating seismic demands and performance based design of the structures for such bracings.

Acknowledgments

The authors would like to use this opportunity to appreciate Khajeh Nasir Toosi University of Technology for supporting this research effectively.

References

[1] ATC. Tentative provisions for the development of seismic regulations for buildings. ATC-3–06. Redwood City, CA: Applied Technology Council; 1978 45–53.
[2] ATC. Structural response modification factors. ATC-19. Redwood City, CA: Applied Technology Council; 1995 5–32.
[3] ATC. A critical review of current approaches to earthquake-resistant design. ATC-34. Redwood City, CA: Applied Technology Council; 1995 31–6.
[4] BHRC. Iranian code of practice for seismic resistance design of buildings: standard no. 2800. 3rd ed. Building and Housing Research Center; 2005.
[5] MHUD. Iranian National Building Code, part 10, steel structure design. Tehran (Iran): Ministry of Housing and Urban Development; 2008.
[6] Kazemi M, ErfaniGargari S. Design of gate bracing system against earthquake. 3rd National Conference of Assessment of Seismic Resistance Design of Buildings Code: Standard No. 2800. Tehran, Iran: BHRC Publication, Building and Housing Research Center; 2002. p. 425–33.
[7] Majid Zamani S, Rasouli M. Numerical and experimental comparison of concentric bracings. BHRC Publication No.R-518. Building and Housing Research Center; 2009.
[8] Saffari H, MosalmanYazdi H. An efficient and direct method for out-of-plane buckling analysis for Y-braced steel frames. J Constr Steel Res 2010;66:1107–11.
[9] Vamvatsikos D, Cornell CA. Incremental dynamic analysis. Earthq Eng Struct Dyn 2002;31(3):491–514.
[10] FEMA. Recommended seismic design criteria for new steel moment frame buildings. Federal Emergency Management Agency Report No. 350; 2000.
[11] Uang CM. Establishing R or (R_w) and C_d factor building seismic provision. J Struct Eng 1991;117(1):19–28.
[12] Uniform building code. Whitter, California: International Conference of Building Officials; 1997.
[13] Mwafy AM, Elnashai AS. Calibration of force reduction factors of RC buildings. J Earthq Eng 2002;6:239–73.
[14] Massumi A, Tasnimi AA, Saatcioglu M. Prediction of seismic overstrength in concrete moment resisting frames using incremental static and dynamic analysis. 13th World Conference on Earthquake Engineering, Vancouver, B.C, Canada; 2004 [Paper No.2826].
[15] Bayat V, Hosseini M, Hosseinzadeh N. Comparison of nonlinear behavior of gate bracing and centric bracing systems. 5th International Conference on Seismology and Earthquake Engineering (SEE 5). Tehran, Iran: International Institute of Earthquake Engineering and Seismology Publication; May 2007. p. 146–55.
[16] Mazzoni S, McKenna F, Scott MH, Fenves GL, Jeremic B. Opensees command language manual; 2007.
[17] Asgarian B, Aghakouchack AA, Bea RG. Inelastic postbuckling and cyclic behavior of tubular braces. J Offshore Mech Arct Eng 2005;127:256–62.